Computation of shear viscosity of colloidal suspensions by SRD-MD

A. M. K. Laganapan, A. Videcoq, M. Bienia, T. Ala-Nissila, D. Bochicchio, and R. Ferrando

Citation: The Journal of Chemical Physics **142**, 144101 (2015); doi: 10.1063/1.4917039
View online: http://dx.doi.org/10.1063/1.4917039
View Table of Contents: http://scitation.aip.org/content/aip/journal/jcp/142/14?ver=pdfcov
Published by the AIP Publishing

Articles you may be interested in

Performance of mesoscale modeling methods for predicting rheological properties of charged polystyrene/water suspensions
J. Rheol. **56**, 353 (2012); 10.1122/1.3690105

Effect of confining conduit on effective viscosity of dilute colloidal suspension
J. Chem. Phys. **132**, 114114 (2010); 10.1063/1.3315867

Shear thickening in a model colloidal suspension
J. Chem. Phys. **123**, 074707 (2005); 10.1063/1.2007667

Computer Simulations of Two Kinds of Polydisperse Hard-Sphere Systems; Atomic Systems and Colloidal Suspensions
AIP Conf. Proc. **708**, 166 (2004); 10.1063/1.1764106

Viscosity equation for concentrated suspensions of charged colloidal particles
J. Rheol. **41**, 769 (1997); 10.1122/1.550875

This article is copyrighted as indicated in the article. Reuse of AIP content is subject to the terms at: http://scitation.aip.org/termsconditions. Downloaded to IP: 130.251.200.3 On: Wed, 08 Apr 2015 14:52:15

Computation of shear viscosity of colloidal suspensions by SRD-MD

A. M. K. Laganapan,[1] A. Videcoq,[1,a)] M. Bienia,[1] T. Ala-Nissila,[2,3] D. Bochicchio,[4] and R. Ferrando[4]
[1]*SPCTS, UMR 7315, ENSCI, CNRS, Centre Européen de la Céramique, 12 rue Atlantis, 87068 Limoges Cedex, France*
[2]*COMP CoE at the Department of Applied Physics, Aalto University School of Science, P.O. Box 11000, FIN-00076 Aalto, Espoo, Finland*
[3]*Department of Physics, Brown University, Providence, Rhode Island 02912-1843, USA*
[4]*Dipartimento di Fisica and CNR-IMEM, via Dodecaneso 33, Genova I-16146, Italy*

(Received 22 December 2014; accepted 26 March 2015; published online 8 April 2015)

The behaviour of sheared colloidal suspensions with full hydrodynamic interactions (HIs) is numerically studied. To this end, we use the hybrid stochastic rotation dynamics-molecular dynamics (SRD-MD) method. The shear viscosity of colloidal suspensions is computed for different volume fractions, both for dilute and concentrated cases. We verify that HIs help in the collisions and the streaming of colloidal particles, thereby increasing the overall shear viscosity of the suspension. Our results show a good agreement with known experimental, theoretical, and numerical studies. This work demonstrates the ability of SRD-MD to successfully simulate transport coefficients that require correct modelling of HIs. © *2015 AIP Publishing LLC.* [http://dx.doi.org/10.1063/1.4917039]

I. INTRODUCTION

Colloidal suspensions have a wide range of applications, ranging from commercial products and industrial processes to biological systems. Of particular significance for many of these systems is the ability to tune and optimize the transport properties of the colloids to obtain the desired flow behaviour. Colloidal suspensions are complex fluids and their rheological response is highly sensitive to thermodynamic parameters, flow geometry, and the underlying microscopic interactions.[1] Resolving the interplay between all of these variables is therefore of great importance for many technological applications.

A characteristic feature of colloidal suspensions is the huge separation of time scales (of the order of $\sim 10^8$) and length scales (of the order of $\sim 10^4$) between mesoscopic colloids and microscopic fluid. Typical quantities of interest are macroscopic transport coefficients that are defined through the relevant fluctuating microscopic variables such as the local density and velocity.[2] Thus, the challenge in understanding the dynamics of colloidal suspensions lies in resolving the huge gap of time and length scales. While experimental studies have revealed several important characteristics of colloidal suspensions, such as shear thinning, shear thickening,[3,4] and yield stress,[5] probing the underlying molecular-level details is either experimentally impossible or expensive. In addition to this, theoretical models are also limited to suspensions with a simplified definition of the fluid. For instance, the results of Einstein[6,7] and Batchelor and Green[8] for transport coefficients are already established for dilute and semi-dilute hard-sphere suspensions but there are no unifying empirical equivalents for concentrated suspensions.[9–11]

Because of the limitations of experimental and analytical approaches, especially for sheared and dense cases, simulations play an increasingly important role in the study of complex fluids. Numerical methods can be used to isolate and analyze the effects of microstructure, composition, geometry, and external perturbation that otherwise cannot be accessed by standard experiments.[12] Over the past years, numerical studies have brought significant contributions to our understanding of flow behaviour and dynamics of colloidal suspensions. However, owing to the disparate nature of the length and time scales of mesoscopic systems, the prediction of rheological coefficients from a microscopic standpoint remains an arduous task. Even with the increasing computer power, a full molecular dynamics (MD) treatment of all the interactions present in the system is still computationally unsustainable. Due to the high complexity of these problems, developing an advanced mesoscopic simulation technique that can address the aforementioned challenges is still a subject of ongoing research.

Most methods available to model suspensions either have an idealized description of the fluid or ignore one of the two important aspects of suspension rheology: thermal fluctuations and hydrodynamic interactions (HIs). A traditional numerical tool for colloidal suspensions is Brownian dynamics (BD), where the fluid is treated as a continuum medium and is represented by frictional and random forces. Despite its success in modelling complex systems, the basic formulation of BD does not include hydrodynamic modes.[13,14] Incorporating HIs in BD in a simplified way requires the use of hydrodynamic tensors such as the BD-Yamakawa-Rotne-Prager (BD-YRP) tensors.[15,16] However, the validity of BD-YRP is constrained to relatively dilute suspensions. In addition, the computational cost increases drastically with increasing number of Brownian particles N since BD-YRP requires tensor evaluation that scales as $O(N^2)$ and diagonalization that scales as $O(N^3)$.

Alternative tools are being developed to address the gap of modelling HIs in mesoscopic simulations. Examples of these

a)arnaud.videcoq@unilim.fr

 © 2015 AIP Publishing LLC

This article is copyrighted as indicated in the article. Reuse of AIP content is subject to the terms at: http://scitation.aip.org/termsconditions. Downloaded to IP: 130.251.200.3 On: Wed, 08 Apr 2015 14:52:15

techniques are Lattice-Boltzmann (LB),[17,18] Dissipative Particle Dynamics (DPD),[19] and Stochastic Rotation Dynamics (SRD),[20–22] which is otherwise known as Multi-Particle Collision (MPC) dynamics. All of these models employ a similar approach, i.e., to coarse-grain the fluid so that the temporal and spatial scales of the fluid are smaller than those of colloids but larger than its own natural scales. In the LB treatment of the fluid, the Boltzmann equation is fully discretized and solved on a lattice. In its original formulation by Ladd,[17,18] thermal fluctuations are not included and artificial Langevin noise terms have to be added to the colloids to restore thermal fluctuations. An improved Fluctuating Lattice-Boltzmann (FLB) model for extended particles with well-defined hydrodynamic radii and without the external Langevin noise has been successfully implemented by Ollila *et al.*[23] This improved method has been introduced and benchmarked for dense and spatially confined systems.

DPD is another popular simulation tool for complex fluid applications because it serves as an augmented version of MD.[19] It is a particle-based approach so that the thermal fluctuations are inherently described. However, describing the fluid using DPD can be computationally demanding when dealing with larger systems since the solvent particles interact through pair-wise potentials.

Stochastic rotation dynamics-molecular dynamics (SRD-MD) is a particle-based approach first introduced by Malevanets and Kapral in 1999.[20] The simplicity of its algorithm has allowed the derivation of analytic expressions for transport coefficients of pure fluids.[24,25] It can successfully reproduce thermal fluctuations and HIs.[26] Of equal importance is that SRD-MD is fast and computationally efficient even for cases that require dealing with external shear and high densities.[27] Recent studies have also shown that it can successfully predict transport coefficients of colloidal suspensions like diffusion coefficient[28–30] and conductivity[31] However, the significance of HIs on diffusion coefficient and conductivity is limited if compared with its relevance on viscosity.

Calculating the shear viscosity of a suspension is a model problem for studying the rheological behaviour of mesoscopic systems.[1,32] Specifically, there have been plenty of studies of suspension viscosity as a function of the particle concentration. It is a key parameter for investigating experimental phenomena such as phase transitions and yield stress. Moreover, theoretical models with concentration as its parameter are well-known[6–8,10] so that it can be used as a benchmark to validate an evolving numerical model. Once validated, one can easily shift to analyze the dependence of shear viscosity on other relevant variables such as shear rate, particle structure, Peclet number (Pe), and Reynolds number (Re).

We limit our study to hard-sphere interactions mainly because their properties are theoretically and numerically well-known as compared to systems with more complex interactions. While it has been shown in Ref. 33 that SRD-MD can be used to calculate viscosity using a Derjaguin, Landau, Verwey and Overbeek (DLVO) potential description for colloid-colloid interaction, we need to justify that the computation of shear viscosity using SRD-MD agrees with existing theoretical predictions and can reproduce results that are comparable with other simulation techniques. The shear viscosity versus volume fraction is a relation that any good numerical method should satisfy. To do this, employing a hard-sphere description of the colloids is sufficient and more practical.

The objective of this paper is to provide a quantitative test on the ability of SRD-MD to model HIs on colloidal suspensions by calculating its shear viscosity. We show that SRD-MD can be used for dilute and concentrated cases. We then compare the results with known theoretical predictions and experimental data. We also propose a method that is different from Refs. 33–35 for calculating shear viscosity. We use a modified version of the SRD-MD stress tensor presented in Ref. 36, a formulation that resembles the virial equation of molecular systems. For this reason, our method of calculation allows for a better characterization of the suspension properties. Moreover, in contrast to Ref. 33 where colloids are treated as point-like particles, we employ a central-force coupling scheme to have a more realistic description of the colloid-fluid dynamics.

The paper is organized as follows. In Sec. II A, we present the system and the simulation procedure. In particular, we describe the MD-treatment of the colloids employed, SRD-treatment of the fluid, and the coupling of the two methods. In Sec. II B, we show how the parameters are chosen to achieve a proper coarse-grained approach. In Sec. II C, we explain how a planar Couette flow is modeled. We also present how the thermostat is implemented, an important point if we want to maintain the correct fluid dynamics while pumping shear. We then proceed to the calculation of relevant quantities. Section III A provides the details of formulating the stress tensors, the main ingredient for obtaining shear viscosity. In Sec. III B, we examine our results for the shear viscosity of the colloidal suspensions and compare them with theoretical equations, numerical models, and experimental data.

II. SIMULATION METHOD

A. The hybrid SRD-MD model

Our system consists of silica spheres ($\rho_c = 2200\ \mathrm{kg\,m^{-3}}$) of radius $a_c = 300\ \mathrm{nm}$ embedded in water ($\rho_f = 1000\ \mathrm{kg\,m^{-3}}$). The SRD parameters and particle interactions implemented in this work are the same as in Ref. 29. The colloids are described by an inverse-power potential that is commonly used for hard-sphere colloids,[28,37]

$$V_{cc} = \begin{cases} \varepsilon_{cc}\left(\dfrac{\sigma_{cc}}{r}\right)^{12} & (r < r_{cc}) \\ 0 & (r > r_{cc}) \end{cases}, \tag{1}$$

where r is the distance between particles, $\sigma_{cc} = 2a_c = 600\ \mathrm{nm}$ is the interaction parameter between colloids, $\varepsilon_{cc} = 2.5k_BT$ and $r_{cc} = 2.5\sigma_{cc}$ is the cutoff distance. The mass of the colloid is obtained from ρ_c and has a value of $M_c = 2.49 \times 10^{-16}$ kg.

For the MD part, the positions and velocities of the colloids are updated at each time step Δt_{MD} using Newton's equation of motion,

$$\mathbf{v}_i = \frac{d\mathbf{r}_i}{dt} \quad \text{and} \quad m_i \frac{d\mathbf{v}_i}{dt} = \mathbf{F}_i. \tag{2}$$

This article is copyrighted as indicated in the article. Reuse of AIP content is subject to the terms at: http://scitation.aip.org/termsconditions. Downloaded to IP: 130.251.200.3 On: Wed, 08 Apr 2015 14:52:15

The positions and velocities are evaluated using the velocity Verlet algorithm.

The fluid dynamics is described using SRD. The fluid is represented by N_f point particles placed in a simulation box of side length L. The SRD process consists of repeatedly streaming and colliding the fluid particles at Δt_{SRD} intervals. During the streaming step, the positions are updated using

$$\mathbf{r}_i(t + \Delta t_{\mathrm{SRD}}) = \mathbf{r}_i(t) + \mathbf{v}_i(t)\Delta t_{\mathrm{SRD}}, \tag{3}$$

where $\mathbf{r}_i$ and $\mathbf{v}_i$ are the ith particle's position and velocity, respectively. In the collision step, the simulation box is divided into smaller cells ($L = 32a_0$) so that each cell has a volume of a_0^3 and contains an average of γ fluid particles. Particle exchanges between cells are allowed but the number of fluid particles in the simulation box is conserved. The collision per cell is performed by rotating the velocities of the particles relative to the center of mass velocity $\mathbf{v}_{\mathrm{cm}}$ according to

$$\mathbf{v}_i(t + \Delta t_{\mathrm{SRD}}) = \mathbf{v}_{\mathrm{cm}} + \mathbf{R}(\alpha)\left[\mathbf{v}_i(t) - \mathbf{v}_{\mathrm{cm}}\right], \tag{4}$$

where $\mathbf{R}$ is the rotation matrix. The coarse grained SRD parameters include the cell size $a_0 = a_c/2 = 150$ nm, the rotation angle $\alpha = 90°$, the average number density $\gamma = 5$, and dimensionless mean-free path $\lambda = 0.1$. All of these parameters are chosen to provide a compromise between resolution and computational cost. The mass of the individual particles is obtained from ρ_f and has a value of $m_f = 6.75 \times 10^{-19}$ kg. The unit of time t_0, which dictates the values of Δt_{SRD} and Δt_{MD}, requires a more thorough discussion and is the subject of Sec. II B.

In the paper by Ihle and Kroll,[25] the authors showed that sorting the fluids fails to satisfy the molecular chaos and Galilean invariance assumptions. This happens when the dimensionless mean-free path, i.e., the average fraction of a cell travelled by a fluid particle during a streaming step is small ($\lambda \ll 1$). This can be solved by using a grid-shift procedure. This is done by constructing a new cell-grid that is randomly translated at a certain distance before each collision step. Collisions are performed in the shifted cells, thus, allowing the exchange of particles. Particles are then reverted back to the original cells and the SRD process is continued.

The colloid-fluid dynamics can be described either by SRD as in Refs. 33, 38, and 39, where the colloids are treated as point particles from the point of view of the fluid particles or by MD, where the colloids have a non-vanishing size. Reference 31 explored the differences between the two coupling schemes and found that the effects of HIs on diffusion coefficient and conductivity are more pronounced when MD is used. Therefore, a MD coupling scheme is more suitable for the calculation of shear viscosity. The coupling proceeds by summing the three different types of interactions present in the colloidal suspension: interactions between colloids that occur at MD time scale (Δt_{MD}), interactions between fluid particles that occur at SRD time scale (Δt_{SRD}), and interactions between colloids and fluid particles that occur at MD time scale. The fluid-fluid interaction potential V_{ff} is set to zero. Hence, the interactions among fluid particles are solely described by SRD. For the dynamics between colloids and fluids, we use an inverse-power potential,

$$V_{cf} = \begin{cases} \varepsilon_{cf}\left(\dfrac{\sigma_{cf}}{r}\right)^{12} & (r < r_{cf}), \\ 0 & (r > r_{cf}) \end{cases} \tag{5}$$

where $\varepsilon_{cf} = 2.5k_BT$ and $r_{cf} = 2.5\sigma_{cf}$.

The consequences of this choice of coupling are as follows. First, it is important to choose σ_{cf} to be slightly less than the colloid radius a_c to avoid unphysical depletion attraction between colloids. Depletion forces are due to spurious interactions that arise from the coarse-grained nature of the fluid when colloids approach each other at short distances.[40,41] In this work, $\sigma_{cf} = 0.8a_c$ is implemented. Subsequently, the fluid particles can slightly penetrate the surface of the colloids. Even when the colloids are in contact, the fluid particles can slide between the colloids, thus, adding lubrication to colloid-colloid interactions. While the MD coupling scheme is more complete in describing colloid-fluid interaction in comparison to the SRD coupling scheme, it does not model angular momentum transfer between colloids and fluid particles leading to an effective slip-boundary condition. The friction coefficient is $\zeta = 4\pi\eta a_c$ for slip-boundary conditions and $\zeta = 6\pi\eta a_c$ for stick-boundary conditions. A stick boundary condition can also be implemented but with an increase of computational cost.[42–44] Second, the free volume accessible to the fluid particles is now dictated by σ_{cf} rather than a_c. This is defined by $V_f = (32a_0)^3 - N_c\frac{4}{3}\pi\sigma_{cf}^3$, where N_c is the number of embedded colloids. In addition, we know from Ref. 29 that the Schmidt number (Sc) of the fluid increases with increasing number of colloids. To keep Sc constant with increasing volume fraction, the number of fluid particles is decreased according to V_f, i.e.,

$$N_f = 32^3\gamma - N_c\frac{4}{3}\pi\left(\frac{\sigma_{cf}}{a_0}\right)^3\gamma. \tag{6}$$

We are now in the position to define the volume fraction occupied by the colloids,

$$\phi = \frac{N_c}{L^3}\frac{4}{3}\pi {r_H}^3, \tag{7}$$

where r_H is the hydrodynamic radius. This is equal to the hard-sphere radius a_{hs} only in the ideal case when there is no explicit fluid present. Analytical approaches to calculate viscosity often deal with an ideal system, where a_{hs} is well defined. However, defining r_H is difficult in simulations and experiments. A hard-sphere approximation requires an inverse-power potential with $n \to \infty$ in Eqs. (1) and (5) instead of $n = 12$, which will require a more expensive calculation. Moreover, the effective r_H for SRD-MD is dependent on several factors including length scale and shear. This is discussed in Refs. 40 and 45 for slip boundary conditions at the colloid-fluid interface. Experimental measurements of ϕ are not simple either. Reference 46 provides an extensive review on the difficulties encountered when measuring ϕ in hard-sphere colloids and the unavoidable uncertainties associated with its reported value. To this point, we have defined two radii for the implementation of SRD-MD: $\sigma_{cc}/2 = a_c$ for the colloid-colloid interaction and $\sigma_{cf} = 0.8a_c$ for the colloid-fluid interaction. In this study, Eq. (7) is evaluated using σ_{cf} because

This article is copyrighted as indicated in the article. Reuse of AIP content is subject to the terms at: http://scitation.aip.org/termsconditions. Downloaded to IP: 130.251.200.3 On: Wed, 08 Apr 2015 14:52:15

TABLE I. Number of colloids and fluid particles corresponding to each volume fractions used in the simulation. These are obtained with $L = 32a_0$ and $a_{hs} = \sigma_{cf} = 0.8a_c$ in Eq. (7).

ϕ	N_c	N_f
0.0513	98	155 433
0.1026	196	147 026
0.1534	293	138 705
0.1791	342	134 501
0.2053	392	130 212
0.2356	450	125 236
0.2618	500	120 947
0.2880	550	116 657
0.3142	600	112 368
0.3388	647	108 336

it is the best r_H approximation for our simulations.[40] Our treatment of volume fraction is similar to the definition used in Ref. 45 for colloid sedimentation velocity, where the volume fraction is defined using r_H instead of σ_{cc}. This is equivalent to viewing the volume fraction from the fluid particle's point of view instead of the colloid's point of view. This will be discussed further in Sec. III B. Table I summarizes the number of colloids and fluid particles used for each volume fraction.

B. SRD mapping

The mesoscopic nature of colloidal suspensions results to a wide range of time scales. SRD-MD compresses this hierarchy of time scales so that only one time scale can be accurately reproduced. We choose from the two significant time scales for this study: kinematic time scale for hydrodynamic interactions and diffusion time scale for Brownian motion. The kinematic time $\tau_\nu = a_c^2/\nu_{H_2O} = a_c^2\rho_f/\eta_{H_2O} = 9.0 \times 10^{-8}$ s and diffusion time $\tau_D = a_c^2/D_0 = 0.12$ s are 6 orders of magnitudes apart. These are obtained using the viscosity of water $\eta_{H_2O} = 0.001$ Pa s and the diffusion coefficient of a colloid in water $D_0 = k_BT/(6\pi\eta_{H_2O}a_c) = 7.15 \times 10^{-13}$ m^2 s^{-1}. Mapping to one of the time scales is necessary to efficiently simulate these transport coefficients. SRD-MD gives the liberty of selecting the fastest time scale to optimize the simulation. In this system, mapping to diffusion time scale will bring the value of τ_ν closer to τ_D, i.e., 6.0×10^{-3} s instead of 9.0×10^{-8} s. However, contracting the time scale results to quantities that are far from laboratory values. For example, the value of shear viscosity will now be 1.52×10^{-8} Pa s for the pure fluid case. When mapped back to kinematic time, the physical value of viscosity is recovered. As mentioned in Ref. 40, the quantitative value is not important as long as the correct regime of the hydrodynamic numbers is obtained and the different time scales are well separated. The diffusion time scale is used in this study because it significantly reduces the computation time by allowing the use of bigger time steps. Hence, longer time scales can be reached at faster rates. Moreover, while the simulated value of shear viscosity is different from its physical value, expressing it in terms of its relative value still preserves all its qualitative features: $\eta_r = \eta_s/\eta_0$. This means that we get the same ratio between the suspension viscosity η_s and pure fluid viscosity η_0 regardless of the time scale used.

By adopting the diffusion time scale, the diffusion time can be expressed as a function of the SRD time unit t_0. A detailed derivation can be found in Ref. 29. Equating the diffusion time in the simulation to the physical value of diffusion time, we get $t_0 = 7.37 \times 10^{-4}$ s. Thus, the SRD time step is $\Delta t_{SRD} = \lambda t_0 = 7.37 \times 10^{-5}$ s. If instead the kinetic time scale is used, the resulting unit of time is $t_0 = 1.12 \times 10^{-8}$ s. This option significantly reduces the computation time by up to 10^4. The value of Δt_{MD} is smaller and generally depends on the steepness of the potential. It was found that $\Delta t_{MD} = \Delta t_{SRD}/8$ is sufficient to resolve the correct Newtonian dynamics for the inverse-power potential used in this paper.

Consequently, the value of temperature is also modified. Similar to the transport coefficients, the actual temperature is mapped from experimental scale to SRD scale and vice versa. A system temperature of 293 K is equivalent to a SRD temperature of

$$T = \frac{a_0^2 m_f}{k_B t_0^2} = 2.02 \times 10^{-3} \text{ K}. \tag{8}$$

A detailed mapping procedure for slip-boundary condition can be found in Refs. 29 and 40.

C. Introducing shear and thermostat

The initial velocities of the particles obey a Maxwell-Boltzmann distribution. The infinite periodic system is then subjected to a uniform shear in the xy plane. Shear is applied in the y direction and the gradient is along the x direction. The shear rate is defined as

$$\dot{\gamma} = \frac{\Delta v_y}{\Delta x}, \tag{9}$$

where Δv_y is the shear velocity. Shear is imposed by using Lees-Edwards boundary conditions (LEBCs),[47] which allows the simulation of a planar Couette flow without actual boundaries. The benefit of using this algorithm is that it does not have the numerical instabilities associated with introducing actual walls. The process works by updating the positions and velocities of the particles with the usual periodic boundary conditions for y and z directions. However, when a particle crosses the upper or lower boundaries of the simulation box, i.e., at $r_x = 0$ and $r_x = L_x$, its position and velocity are updated with a different rule to sustain the shear. Particles crossing the upper boundary will have an additional velocity of $+\dot{\gamma}L_x$ and a position shift of $+\dot{\gamma}L_x t$, where t is the total elapsed time. In contrast, particles crossing the lower boundary will have an additional velocity of $-\dot{\gamma}L_x$ and a position shift of $-\dot{\gamma}L_x t$. LEBCs are applied for both the colloids and fluid particles.

A shear rate of $\dot{\gamma} = 100$ s^{-1} is used and gives the system Pe = 12.6. Viscosity is measured when the velocity profile is already linear. Fig. 1 shows the velocity profile inside a simulation box for a suspension with $\dot{\gamma} = 100$ s^{-1} and $\phi = 0.1534$.

The introduction of shear results to continuous pumping of external energy into the system. The kinetic energy of the system is kept constant by applying a thermostat. The instantaneous kinetic temperature of the system is defined as

This article is copyrighted as indicated in the article. Reuse of AIP content is subject to the terms at: http://scitation.aip.org/termsconditions. Downloaded to IP: 130.251.200.3 On: Wed, 08 Apr 2015 14:52:15

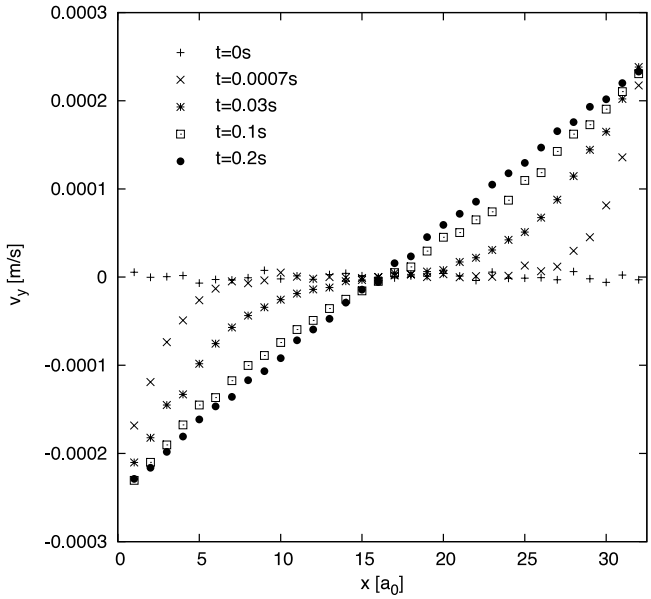

FIG. 1. Velocity profile for $\phi = 0.1534$ and a shear rate of $\dot{\gamma} = 100\ \mathrm{s}^{-1}$. A linear profile is observed at 0.2 s.

$$\mathcal{T} = \frac{1}{k_B d} \sum_{i=1}^{N} m_i (v_i - u_{\dot{\gamma}})^2, \tag{10}$$

where $d = 3$ is the dimensionality and $u_{\dot{\gamma}}$ is the simulated shear velocity. A constant temperature is maintained by using a Monte Carlo scaling thermostat.[26,48] Several types of thermostats have been employed and Monte Carlo scaling proves to be the most efficient. This method also conserves linear momentum and energy without smearing the velocity profile or changing the viscosity of the fluid. The SRD coupling in Refs. 26 and 33 also changes the temperature of the colloids because they participate to the SRD collision steps. In our case, the thermostat is only applied to the fluid particles. Hence, the interaction of the colloid with the thermal bath happens only during colloid-fluid interactions. The thermostat described has been tested for shear rates between 10 s^{-1} and 500 s^{-1}.

An equilibration part consisting of 2000 – 6000 SRD steps is first carried out. This is the part where $\mathcal{T}$ is slowly driven to the desired T. This approach is needed to ensure that the viscosities are measured with the correct linear velocity profile and at the correct system temperature.

III. CALCULATIONS

A. Stress tensors

The viscosity is obtained from $\eta = \langle \sigma_{yx} \rangle / \dot{\gamma}$, where $\langle \ldots \rangle$ denotes a time average. We use the instantaneous stress tensors from Ref. 36 and adapt it for our system. For the pure fluid case ($\phi = 0$), these are given by

$$\sigma_{\mathrm{kin},yx} = -\frac{m_f}{V} \sum_{i=1}^{N_f} \hat{v}'_{iy} \hat{v}_{ix} - \frac{m_f \dot{\gamma} \Delta t_{\mathrm{SRD}}}{2V} \sum_{i=1}^{N_f} v_{ix}^2 \tag{11}$$

and

$$\sigma_{\mathrm{col},yx} = -\frac{1}{V \Delta t_{\mathrm{SRD}}} \sum_{i=1}^{N_f} \Delta p_{iy} r'_{ix}, \tag{12}$$

where $V = L^3$ for the pure fluid case and the shorthand notations $\hat{v}_\alpha = v_\alpha(t - \Delta t)$ and $\Delta p_{iy} = m_f(v_{iy} - \hat{v}_{iy})$ are used. The apostrophe symbol ($'$) is for quantities measured after LEBCs are imposed. Equations (11) and (12) correspond to the kinetic and collisional contributions, respectively, so that the total stress tensor of the fluid is $\sigma_{yx}^{\mathrm{fluid}} = \sigma_{\mathrm{kin},yx} + \sigma_{\mathrm{col},yx}$. Viscosity is calculated for r'_{ix} before and after imposing the grid-shift procedure. We found that an agreement with the known analytical fluid viscosity is obtained when r'_{ix} is measured after the grid-shifting algorithm. We compared them with the analytical predictions for the shear viscosity of pure fluids as a function of SRD parameters,[24,25]

$$\eta_{\mathrm{kin}} = \frac{5\gamma^2 k_1}{(\gamma - 1 + e^{-\gamma})(4 - 2\cos\alpha - 2\cos 2\alpha)} - \frac{1}{2}\gamma k_1, \tag{13}$$

$$\eta_{\mathrm{col}} = k_2(1 - \cos\alpha)(\gamma - 1 + e^{-\gamma}), \tag{14}$$

where $k_1 = k_B T \Delta t_{\mathrm{SRD}} / a_0^3$, $k_2 = m/(12 a \Delta t_{\mathrm{SRD}})$, and $\eta_{\mathrm{tot}} = \eta_{\mathrm{kin}} + \eta_{\mathrm{col}}$. Since we used a small value for $\lambda = 0.1$, the viscosity is dominated by the momentum transfer from particle collisions and not by the streaming of the fluid. At $\alpha = 90°$, the calculated viscosity is 1.5×10^{-8} Pa s. The same value of shear viscosity is obtained using other approaches.[21,24] The viscosity remains constant between 50 s^{-1} and 100 s^{-1}. This is expected since experimental results show that shear thickening and shear thinning occur at shear rates beyond these values (see Ref. 49).

A small deviation from the theoretical values is seen at higher angles (120°-150°). A similar observation is also found when the method proposed in Ref. 24 is used. This small deviation may be due to (1) the increase in the number of degrees of freedom and (2) the small effect of the coarse-grained temperature (2.02×10^{-3} K). This may lead to a small loss of molecular chaos at low temperatures (see Ref. 24).

Because the simulations of the pure fluid case are in good agreement with analytical equations, we have generalized the above approach to obtain the shear viscosity of colloidal suspensions. We use the stress tensor

$$\sigma_{yx}^{\mathrm{colloid}} = -\frac{M_c}{V} \sum_{i=1}^{N_c} \hat{v}'_{iy} \hat{v}_{ix} - \frac{M_c \dot{\gamma} \Delta t_{\mathrm{SRD}}}{2V} \sum_{i=1}^{N_c} v_{ix}^2 - \frac{1}{V} \sum_{i=1}^{N_c} F_{iy} r'_{ix}. \tag{15}$$

Since the coupling method used in this paper is MD, the colloid forces are explicitly defined. Using Eqs. (1) and (5), F_{iy} is obtained directly from $\partial \left(V_{cc,i} + V_{cf,i}\right) / \partial r_y$ instead of the pseudo force $\Delta p_{i\alpha}$ used in Eq. (12). The total stress tensor of the suspension is calculated from the sum of the contributions from the embedded colloids and suspending fluid,

$$\sigma_{yx}^{s} = \sigma_{yx}^{\mathrm{fluid}} + \sigma_{yx}^{\mathrm{colloid}}. \tag{16}$$

Therefore, $\eta_s = \eta^{\mathrm{fluid}} + \eta^{\mathrm{colloid}}$. The results of five independent simulations are reported and the error bars corresponding to the standard deviations are smaller than the symbols used.

This article is copyrighted as indicated in the article. Reuse of AIP content is subject to the terms at: http://scitation.aip.org/termsconditions. Downloaded to IP: 130.251.200.3 On: Wed, 08 Apr 2015 14:52:15

B. Shear viscosity

For the theoretical framework of shear viscosity, we use Einstein's equation[6,7] for the dilute case and Krieger's semi-empirical equation for the concentrated case.[11] The hard-sphere equations are given by

$$\eta_r = 1 + 2.5\phi \text{ for } \phi \to 0 \tag{17}$$

and

$$\eta_r = \left(1 - \frac{\phi}{\phi_m}\right)^{-p} \text{ for } \phi \to \phi_m, \tag{18}$$

where ϕ_m is the maximum packing fraction and p is a parameter that depends on ϕ_m and the shear. The deviation from the linear approximation is due to the increase of the probability of collisions and because hydrodynamic interactions become more significant at higher volume fractions.[32]

Fig. 2 shows how shear viscosity increases with increasing value of σ_{cf}. The predicted value using Eq. (17) is also shown for comparison. As σ_{cf} approaches a_c, the calculated shear viscosity moves closer to the analytical result. However, in the limit $\sigma_{cf} \to a_c$, depletion attraction starts to occur and the calculated viscosity in this region ($\sim 0.95a_c$) is no longer valid. Cluster formations caused by the depletion attraction are observed when $\sigma_{cf} = a_c$ but are eliminated when $\sigma_{cf} = 0.8a_0$. The result of Fig. 2 justifies the choice of using σ_{cf} as the hydrodynamic radius in Eq. (7).

The shear viscosity of the colloids (η^{colloid}) can also be divided into components owing to the different contributions to the stress tensor. The virial part, described by the last term in Eq. (15) and represented by blue diamonds in Fig. 3, increases because of the increase in the probability of collisions among other colloids when the volume fraction increases. It is also the most dominant contribution to the overall viscosity. The kinetic contribution, described by the first two terms in Eq. (15), is represented by red squares in Fig. 3. It represents the pressure exerted by the colloids on a surface. As expected, it increases with increasing volume fraction. However, it is smaller in comparison to the contribution from the colloid-colloid interactions. The shear viscosity from the colloids is therefore dominated by the momentum exchanges from inter-particle interactions rather than from streaming.

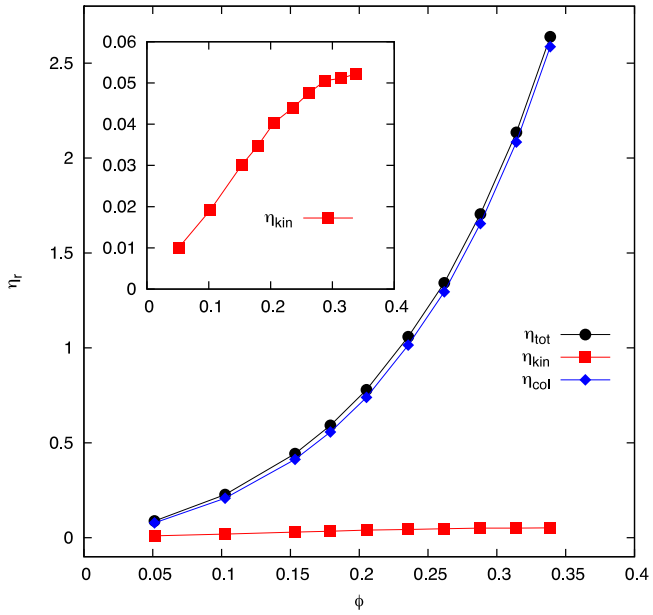

FIG. 3. The shear viscosity contribution from the colloids η^{colloid} (black circles) is comprised of the kinetic part (red squares) and the collisional part (blue diamonds).

We use the same treatment to analyze what is happening to the shear viscosity of the SRD fluid (η^{fluid}) as the volume fraction increases (see Fig. 4). The total shear viscosity (black circles) is comprised of the kinetic part (red squares)

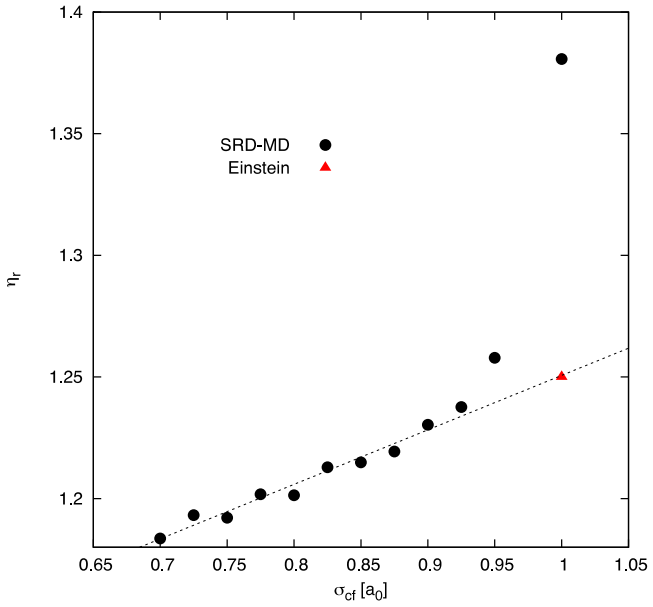

FIG. 2. Dependence of shear viscosity η_r on the interaction parameter σ_{cf} for $\phi = 0.0513$. As σ_{cf} approaches a_c, the viscosity approaches the theoretical value predicted by the Einstein equation, except very close to a_c, where depletion attraction causes an increasing deviation. The line is a guide to the eyes.

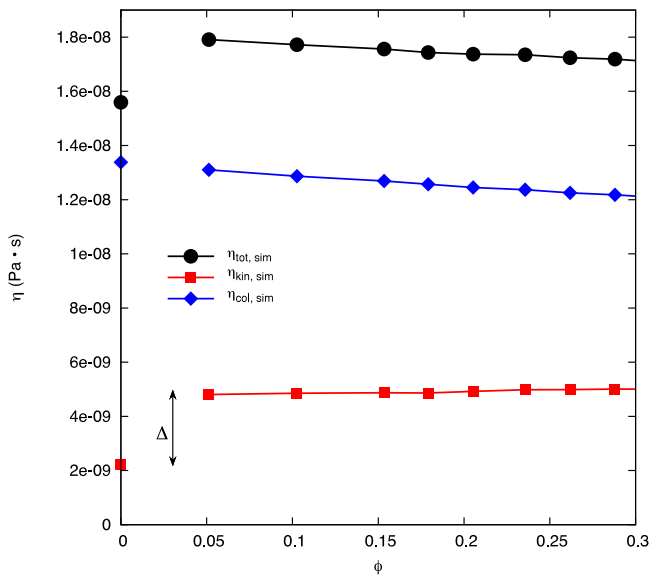

FIG. 4. The shear viscosity contribution of the SRD fluid η^{fluid} is comprised of the kinetic viscosity (red squares) and collisional viscosity (blue diamonds). We also compare the viscosity of the SRD fluid ($\eta^{\text{fluid}}(\phi)$) with the predicted shear viscosity for the pure fluid case ($\eta^{\text{fluid}}(\phi = 0)$) given by Eqs. (13) and (14) from Refs. 24 and 25. An average difference of $\Delta = 2.7 \times 10^{-9}$ Pa s is measured.

This article is copyrighted as indicated in the article. Reuse of AIP content is subject to the terms at: http://scitation.aip.org/termsconditions. Downloaded to IP: 130.251.200.3 On: Wed, 08 Apr 2015 14:52:15

and collisional part (blue diamonds). For the collisional contribution, which describes the collisions among fluid particles, no significant change can be observed. In contrast, the kinetic contribution, which describes the streaming of the fluid particles, increases by $\Delta = 2.7 \times 10^{-9}$ Pa s when colloids are present. This is due to the additional momentum imparted by the fluid-colloid interactions when streaming.

Finally, we compare the suspension viscosity with other known results in Fig. 5. For the experimental part, we compared with the data by Segré[53] and van der Werff,[54] where they used undeformable, sterically stabilized spheres. The volume fraction is approximated using the maximum packing fraction of the system, $\phi_m = 0.494$ for Segré[53] and $\phi_m = 0.63$ for van der Werff.[54] It can be observed that our numerical results lie a little below the experimental data of Refs. 53 and 54. This can be due to finite size effects that make the shear rate higher than the expected value.

Our results are comparable with those of Koelman and Hoogerbrugge,[51,52] where they simulate hard-sphere suspensions under shear flow using DPD. The hard-sphere case is imposed by using the moment of inertia and Euler's equation of motion for rigid bodies.[52]

The behaviour of hard-sphere suspensions in the absence of HIs was analyzed using BD in Ref. 50. In order to remove Pe and volume fraction dependencies of the shear viscosity, Ref. 50 employed an algorithm, in which after the Brownian position updates, the overlaps are checked and successively removed.[55] By comparing the behaviour of the two systems, HIs increase the viscosity of the suspension. In contrast to the BD where the effect of fluid particles is represented by the frictional and stochastic terms, the fluid description in SRD-MD is more explicit. It is observed that the overall contribution of the fluid decreases with increasing volume fraction since the number of fluid particles decreases with increasing concentration to maintain a constant Sc for the fluid. Even so, the treatment of the fluid by SRD-MD provides lubrication between colloid particles because the fluid can slide between them. This increases the chances of collisions among colloids and the overall friction of the system.

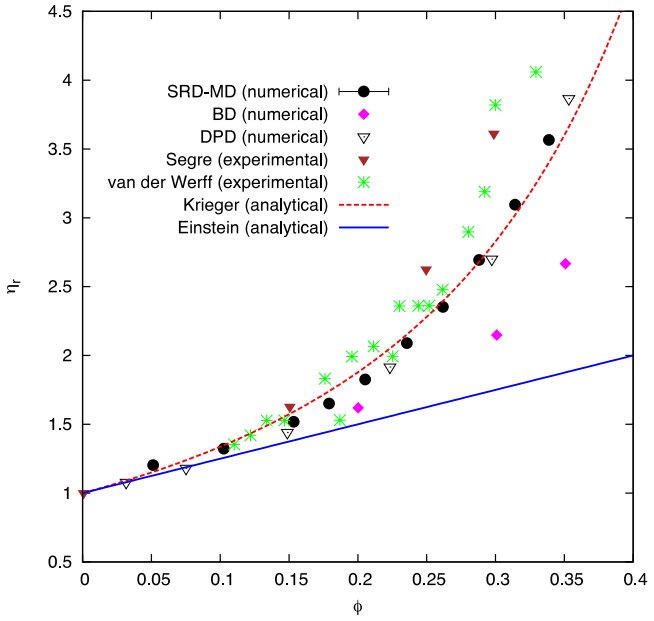

FIG. 5. Relative shear viscosity of the colloidal suspension as a function of volume fraction compared with other numerical,[50–52] experimental,[53,54] and analytical studies.[6,7,11]

From the theoretical standpoint, the results follow Eq. (17) for low volume fractions and start to diverge near $\phi = 0.15$. For Eq. (18), we used a fitting parameter of $\phi_m \sim 0.74$ because the highest packing achievable in our simulation box is hexagonal closed packing. Previous theoretical works have shown that $p = 2$ for a variety of situations[14,56] so that Eq. (18) reduces to $\eta_r = (1 - \phi/0.74)^{-2}$.

IV. CONCLUSIONS

We have demonstrated that SRD-MD can be used to simulate the shear viscosity of colloids. The mapping between physical and simulated values can be done by SRD-MD without losing relevant information. The use of diffusion time scale for computation significantly decreases the simulation time. Shear can also be applied to systems that uses MD as a coupling scheme. A Monte Carlo scaling thermostat is necessary to maintain the correct thermodynamic properties of the fluid.

The choice of σ_{cf} in defining the volume fraction also gives the correct viscosity values. A small σ_{cf} allows more fluid particles to perturb the flow field surrounding the colloid.

The use of stress tensors for viscosity evaluation provides a better characterization tool than what is previously available as in Ref. 33. We observed that the main contribution to the shear viscosity of the suspension comes from the inter-particle collisions rather than streaming. The contribution of the fluid particles to the stress tensor decreases with increasing concentration. This is a consequence of the coupling scheme used and is necessary in order to preserve the Sc of the fluid. However, their role in facilitating lubrication between colloidal particles aids in the increase of kinetic and collisional viscosities of the colloids, which is not seen in simulations neglecting hydrodynamic effects. Our results are also comparable with other experimental and theoretical studies. While results for hard-sphere suspensions employing other methods, like DPD, have been compared to Eqs. (17) and (18), this is the first time that the relation between shear viscosity and volume fraction is reproduced by SRD-MD. Hence, our study serves as a final test on the ability of SRD-MD to predict transport coefficients and rheological parameters where HIs are significant. Moreover, in comparison to DPD, the SRD treatment of the system is computationally faster especially at intermediate and high-volume fractions. SRD-MD is also a practical tool for studying the rheology of dense suspensions, an important aspect for studying yield-stress and other phenomena that are occurring in the non-Newtonian regime.

ACKNOWLEDGMENTS

A.K.L. acknowledges support from the Programme VINCI 2013 of the French-Italian University on the subject "Structuration of ceramic suspensions under constraints". The calculations presented are carried out on CALI, funded by the

This article is copyrighted as indicated in the article. Reuse of AIP content is subject to the terms at: http://scitation.aip.org/termsconditions. Downloaded to IP: 130.251.200.3 On: Wed, 08 Apr 2015 14:52:15

institutes of XLIM, IPAM, GEIST, the University of Limoges and Région Limousin. T.A.-N. has been supported in part by the Academy of Finland through the COMP CoE Grant No. 251748, and by the EXPECTS project at Aalto University.

[1]J. M. Brader, J. Phys.: Condens. Matter **22**, 363101 (2010).
[2]L. E. Reichl and I. Prigogine, *A Modern Course in Statistical Physics* (University of Texas Press, Austin, 1980), Vol. 186.
[3]X. Cheng, J. McCoy, J. Isaraelchvili, and I. Cohen, Science **333**, 1276 (2011).
[4]R. L. Hoffman, J. Rheol. **42**, 111 (1998).
[5]D. V. Boger, Nature **265**, 126 (1977).
[6]A. Einstein, Ann. Phys. **19**, 289 (1906).
[7]A. Einstein, Ann. Phys. **34**, 591 (1911).
[8]G. K. Batchelor and J. Green, J. Fluid Mech. **56**, 401 (1972).
[9]G. Szamel, Chem. Phys. Lett. **114**, 8708 (2001).
[10]R. A. Lionberger and W. B. Russel, J. Chem. Phys. **106**, 402 (1997).
[11]I. M. Krieger and T. J. Dougherty, Trans. Soc. Rheol. **3**, 137 (1959).
[12]B. Dünweg and A. J. C. Ladd, *Advance Computer Simulation Approaches for Soft Matter Sciences III*, 1st ed. (Springer, Berlin, 2009), Chap. 2, p. 91.
[13]D. L. Ermak and A. J. McCammon, J. Chem. Phys. **69**, 1352 (1978).
[14]J. F. Brady and J. F. Morris, J. Fluid Mech. **348**, 103 (1997).
[15]J. Rotne and S. Prager, J. Chem. Phys. **50**, 4831 (1969).
[16]H. Yamakawa, J. Chem. Phys. **53**, 436 (1970).
[17]A. J. C. Ladd, J. Fluid Mech. **271**, 285 (1994).
[18]A. J. C. Ladd, J. Fluid Mech. **271**, 331 (1994).
[19]R. D. Groot and P. Warren, J. Fluid Mech. **107**, 4423 (1997).
[20]A. Malevanets and R. Kapral, J. Chem. Phys. **110**, 8605 (1999).
[21]A. Malevanets and R. Kapral, J. Chem. Phys. **112**, 7260 (2000).
[22]R. Kapral, Adv. Chem. Phys. **140**, 89 (2008).
[23]S. T. T. Ollila, C. Denniston, M. Karttunen, and T. Ala-Nissila, J. Chem. Phys. **134**, 064902 (2011).
[24]N. Kikuchi, M. Pooley, J. F. Ryder, and J. M. Yeomans, J. Chem. Phys. **119**, 6388 (2003).
[25]T. Ihle and D. M. Kroll, Phys. Rev. E **67**, 066705 (2003).
[26]G. Gompper, T. Ihle, D. M. Kroll, and R. G. Winkler, *Advance Computer Simulation Approaches for Soft Matter Sciences III*, 1st ed. (Springer, Berlin, 2009), Chap. 1, pp. 1–88.
[27]A. Nikoubashman, N. A. Mahynski, A. H. Pirayadeh, and A. Z. Panagiotopoulos, J. Chem. Phys. **140**, 094903 (2014).
[28]E. Falck, J. M. Lahtinen, I. Vattulainen, and T. Ala-Nissila, Eur. Phys. J. E **13**, 267 (2004).
[29]A. Tomilov, A. Videcoq, T. Chartier, T. Ala-Nissila, and I. Vattulainen, J. Chem. Phys. **137**, 014503 (2012).
[30]A. Tomilov, A. Videcoq, M. Cerbelaud, M. A. Piechowiak, T. Chartier, T. Ala-Nissila, D. Bochicchio, and R. Ferrando, J. Phys. Chem. B **117**, 14509 (2013).
[31]G. Batôt, V. Dahirel, G. Mériguet, A. Louis, and M. Jardat, Phys. Rev. E **88**, 043304 (2013).
[32]D. B. Genovese, Adv. Colloid Interface Sci. **171-172**, 1 (2012).
[33]M. Hecht, J. Harting, M. Bier, J. Reinshagen, and H. Herrmann, Phys. Rev. E **74**, 021403 (2006).
[34]C. C. Huang, R. Winkler, G. Sutmann, and G. Gompper, Macromolecules **43**, 10107 (2010).
[35]D. A. Fedosov, S. Singh, A. Chatterji, R. Winkler, and G. Gompper, Soft Matter **8**, 4109 (2012).
[36]R. G. Winkler and C. C. Huang, J. Chem. Phys. **130**, 074907 (2009).
[37]H. Löwen, Phys. Rev. E **53**, R29 (1996).
[38]M. Hecht, J. Harting, T. Ihle, and H. Herrmann, Phys. Rev. E **72**, 011408 (2005).
[39]C. M. Pooley and J. M. Yeomans, J. Phys. Chem. B **109**, 65015 (2005).
[40]J. T. Padding and A. A. Louis, Phys. Rev. E **74**, 031402 (2006).
[41]A. A. Louis, E. Allahyarov, H. Löwen, and R. Roth, Phys. Rev. E **65**, 061407 (2002).
[42]J. T. Padding, A. Wysocki, H. Löwen, and A. A. Louis, J. Phys.: Condens. Matter **17**, S3393 (2005).
[43]J. K. Whitmer and E. Luijten, J. Phys.: Condens. Matter **22**, 104106 (2010).
[44]I. O. Götze, H. Noguchi, and G. Gompper, Phys. Rev. E **76**, 046705 (2007).
[45]J. T. Padding and A. A. Louis, Phys. Rev. Lett. **93**, 220601 (2004).
[46]W. K. Poon, E. R. Weeks, and C. P. Royall, Soft Matter **8**, 21 (2012).
[47]A. W. Lees and S. F. Edwards, J. Phys. C: Solid State Phys. **5**, 1921 (1972).
[48]C. C. Huang, A. Varghese, G. Gompper, and R. G. Winkler, Phys. Rev. E **91**, 013310 (2015).
[49]D. Kalman and N. J. Wagner, Rheol. Acta **48**, 897 (2009).
[50]D. R. Foss and J. F. Brady, J. Rheol. **44**, 629 (2000).
[51]J. M. Koelman and P. J. Hoogerbrugge, Europhys. Lett. **21**, 363 (1993).
[52]P. J. Hoogerbrugge and J. M. V. A. Koelman, Europhys. Lett. **19**, 155 (1992).
[53]P. N. Segrè, S. P. Meeker, P. N. Pusey, and W. C. K. Poon, Phys. Rev. Lett. **75**, 958 (1995).
[54]J. van der Werff and C. de Kruif, J. Rheol. **33**, 421 (1989).
[55]D. M. Heyes and J. R. Melrose, J. Non-Newtonian Fluid Mech. **46**, 1 (1993).
[56]D. Quemada and C. Berli, Adv. Colloid Interface Sci. **98**, 51 (2002).

This article is copyrighted as indicated in the article. Reuse of AIP content is subject to the terms at: http://scitation.aip.org/termsconditions. Downloaded to IP: 130.251.200.3 On: Wed, 08 Apr 2015 14:52:15